Experimental Research

10.1 General

A variety of experimental techniques were utilized by researchers in the past to determine load distribution among bolts and strains in the vicinity of the bolt hole. Traditionally strain gages and Moiré interferometry were employed to validate analytical models (Wilkinson and Rowlands 1981, Rowlands et al. 1982, Rahman et al.1991). However, strain gages are sometimes problematic to mount and wire on wood, especially when an increasing number of bolts in a connection is investigated. Other methods such as extensometers, Moiré interferometry, brittle coatings, photoelasticity, and laser speckle interferometry are either not applicable for full-field measurements, require special surface treatments that could affect the mechanical properties of wood, or are simply too costly and tedious.

A relatively new technique to monitor bolt deformations is the ultrasonic pulse-echo inspection technique. This technique employs the theory of wave propagation in cylindrical solids. An ultrasonic impulse, applied at one end of a cylindrical rod, is reflected from and directed by the sidewalls as it traverses the length of the rod. The established knowledge about ultrasonic echo analysis evolved from earlier work done by McSkim (1956), Varey (1976), and Light and Joshi (1986) who developed a cylindrically guide wave technique (CGWT) for inspecting bolts and studs in nuclear power plants. The CGWT makes use of pulse-echo inspection by coupling an ultrasonic transducer to one end of the bolt (Pollock et al. 1996). The resulting ultrasonic signal is then evaluated. Pollock et al. (1996) used this technique for nondestructive evaluation to monitor bolts in timber connections. They correlated ultrasonic signal characteristics with plastic hinge formation in bolted connections. The researchers concluded: "the plastic hinge angle magnitude in bolts can be identified by relative changes in trailing echo amplitudes." The technique is of limited use for joints under cyclic loading, however, for signal interpretation can only be done when the system is at rest. That is, to this end, a continuous, real time signal evaluation has not been developed.

Stelmokas (1995) and Salenikovich et al. (1996) utilized a new experimental technique to monitor the load distribution in multiple-bolt joints under one-directional loading. They used bolts instrumented with internal strain gages that directly measure the shear loads distributed to

each bolt in the connection. Instrumented bolts are essentially load cells designed to function as a conventional bolt and at the same time output an electronic signal directly correlated to the magnitude of the shear forces at the shear planes of the bolts. In the works by Stelmokas and Salenikovich, the specimens were not loaded to failure as the instrumented bolts would have been destroyed. If applied to reversed cyclic loading, the technique is poised to yield erroneous results however, since it cannot be guaranteed that the bolt and hence the strain gages within the bolt stay optimally aligned.

Initially, the experimental phase for this work was intended to complement the analytical study but later developed into a separate project performed by Anderson (2001). Owing to the intricate nature of the experiments, it was desired to keep procedures as simple as possible. This implies that tests were planned to make statistical inferences between single- and multiple-bolt performance rather than using tedious instrumentation designed to study multiple bolt behavior. Procedures, methods and results are briefly described in this chapter. Discussion and inferences drawn focus on the tests conducted relevant for this work only. For more detailed information and information about other tests, the reader is referred to Anderson (2001)).

10.2 Experimental Design

A portion of the experimental plan pertinent to this work is depicted in Table 10.1. The complete version can be found in Anderson (2001). Test specimens were single shear connections and were selected for two reasons: 1) to be representative of connections used in wood construction for drag struts, shear collectors, and connections between diaphragms and concrete walls, and 2) to obtain 3 of the 4 yield modes assumed in the 1991 NDS[1]. Monotonic (unidirectional) displacing tests were necessary to calibrate the cyclic protocol. In addition monotonic tests serve to validate MULTBOLT for a drastically different input function.

Single-bolt configurations serve as control sample to make inferences about multiple-bolt behavior relative to single-bolt performance. Materials of the joint members and their thickness were selected to include Yield Modes II and IV. Bolt spacing was chosen to equal the minimum allowable spacing for full design value published in the NDS, which is four times the bolt diameter (AF&PA 1997). Minimum end and edge distances of all connections tested also complied with minimum distances recommended by the NDS. Tests were conducted with bolt holes drilled at 1.6 mm (1/16-inch) oversize. This tolerance is also consistent with the 1997 NDS.

---

[1] For results of joints designed to yield in Mode III, see Anderson (2001).

Table 10.1: Experimental design

Bolt Diameter (mm)	Side Member Cross Section (mm^2) and Material	Expected Yield Mode	No. of Bolts in a Row	Displacing Protocol	Replications
12.7	89x140 SP	IV	1	monotonic	3
12.7	89x140 SP	IV	3	monotonic	3
12.7	89x140 SP	IV	1	cyclic	10
12.7	89x140 SP	IV	3	cyclic	10
12.7	89x140 SP	IV	5	cyclic	10
12.7	38x140 SP	II	1	monotonic	3
12.7	38x140 SP	II	3	monotonic	3
12.7	38x140 SP	II	1	cyclic	10
12.7	38x140 SP	II	3	cyclic	10
12.7	38x140 SP	II	5	cyclic	10

10.2.1 Sample Size

With the exception of monotonic tests, the number of replications per configuration was determined according to

$$n = \frac{2 z^2_{\alpha/2} \; COV^2}{e^2} \tag{10.1}$$

where

$$COV = \frac{\sigma}{\mu} \tag{10.2}$$

$$e = \frac{\Delta}{\mu} \tag{10.3}$$

		Unit
COV	coefficient of variation	%
σ	standard deviation	same as μ
μ	population mean of any variable	any
e	relative error	%
Δ	absolute error	same as μ
$Z_{\alpha/2}$	area under normal curve associated with a $100(1-\alpha)$% confidence interval	

An upper bound estimate of *COV* may be found utilizing data obtained by Gutshall (1994). Gutshall tested single-bolt joints of several configurations in single shear subjected to Sequential

Phased Displacement loading. The highest *COV* for maximum load was reported to be 16.1 percent for a 19 mm bolt loaded parallel to the grain with 89 x 89 mm^2 (4 x 4 inch^2 nominal) side members. According to this data, a sample size of ten assures with 90 percent confidence that the estimated mean is within 12 percent of the true mean of maximum load.

Monotonic sample size was smaller because the primary purpose of these tests was to calibrate the cyclic protocol and not to make inferences between single- and multiple-bolt response.

10.2.2 Test Apparatus

An MTS servo hydraulic test machine was used to conduct the tests. Test apparatus and fabrication jigs were specifically constructed to provide desired loading and accurate specimen fabrication. The fixture was designed to assure that mostly shear forces are induced and that moments due to asymmetry are minimized at the load cell and in the joint. Steel braces served to absorb horizontal forces and keep specimen and grip aligned. In order to hold each member in place at joint capacity, up to eighty self-drilling Simpson Strong-Drive® wood screws (diameter 6.3 mm) or small diameter lag bolts (diameter 6.3 mm) joined each member with the grips as depicted in Figure 10.1. Displacements of each member were measured relative to the same base using string potentiometers (Figure 10.2).

Load cell

Steel brace

Simpson Strong-Drive ®
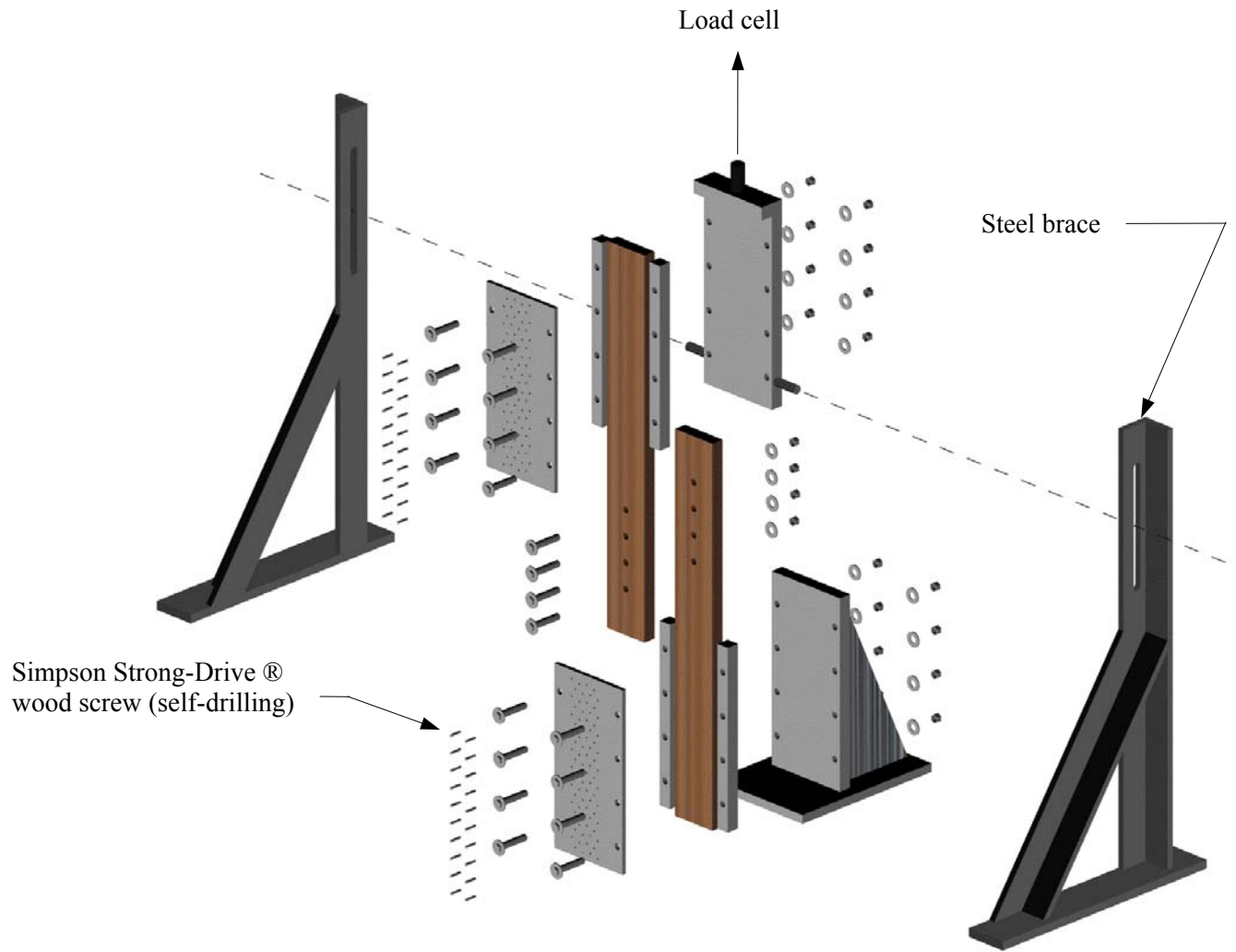wood screw (self-drilling)
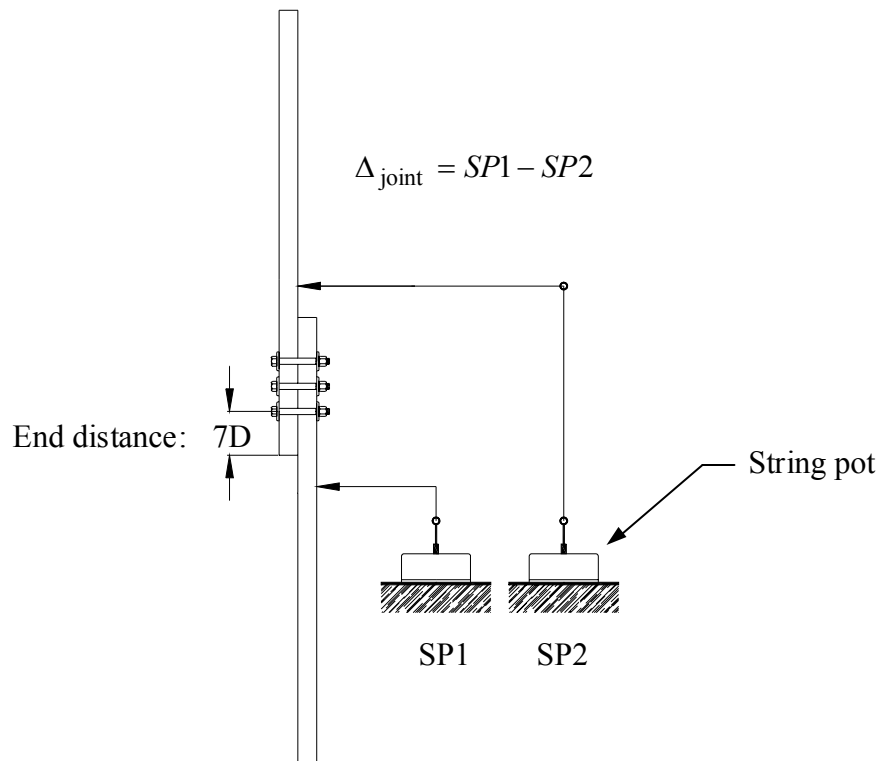
Figure 10.1: Devised test set-up and fixture

Figure 10.2: Displacement measurements. To accurately record the displacements of the two members, two string pots were attached such that the displacement of each member was measured relative to the same base. Total joint displacement is then the difference of the two displacements recorded.

10.3 Test Protocol

Historically, researchers were concerned about the ultimate strength of timber connections. It is therefore not surprising that until recently, the most commonly used testing procedure to evaluate mechanical properties of wood structural systems and connections has been the unidirectional procedure, standardized by the American Society of Testing and Materials (ASTM D1761, ASTM 1997). Scientists have agreed that results of this procedure do not provide sufficient information to evaluate earthquake performance of timber connections and structures (Foliente 1996, Skaggs and Rose 1996, Ceccotti 1995).

Although the first reversed-cyclic load tests on nailed timber joints were conducted more than forty years ago (Kaneta 1958), a standardized procedure to serve as common basis for research and design efforts has not yet been adopted. Many standards are currently being developed, however, and numerous draft standards subject to review exist as of this writing.

The draft standards described below are a combination of unidirectional and cyclic tests. Unidirectional tests are conducted to obtain basic properties that are used to adjust the cyclic test regime if a connection is tested for the first time. All draft standards elaborated below are displacement controlled, which is derived from the fact that true seismic excitation of structures is displacement driven.

10.3.1 Proposed ASTM Standard (7th Draft: cyclic test standard February, 1999)

The proposed ASTM standard is a pseudodynamic load regime and incorporates the concept of the Sequential Phased Displacement (SPD) Procedure, which was developed by the Technical Coordinating Committee on Masonry Research (TCCMAR), a joint earthquake research project between USA and Japan. The procedure was first described by Porter (1987) and later revised by Dolan (1993), Dolan and Johnson (1996b), and the Structural Engineers Association of Southern California (SEAOSC) in 1996. The standard is currently in review process.

In general, the SPD protocol is displacement controlled and involves triangular reversed cyclic loading at incrementally increasing displacement levels (Figure 10.3). The incremental increase is controlled by the experimentally determined displacement at the first major event (FME) of the structure. The FME is defined as the displacement at which the structure starts to deform inelastically (anticipated yield displacement). Unlike the original SPD protocol, which stipulates a quasistatic displacement rate, the cyclic frequency suggested in the ASTM draft is held constant at 0.5 Hz. Note that with a fixed frequency and changing displacement amplitudes the displacement rate is not constant.
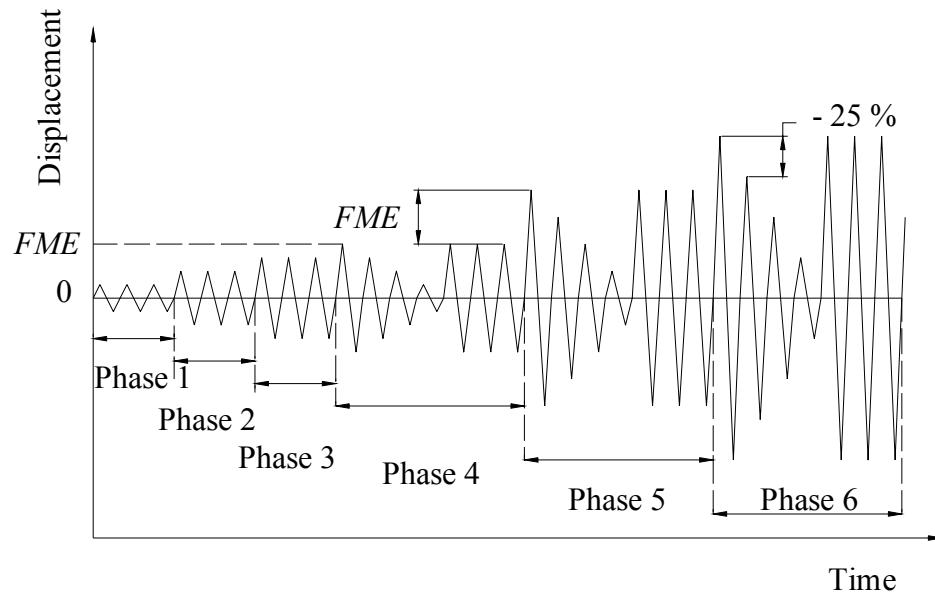
Figure 10.3: Displacement pattern of proposed ASTM standard based on SPD protocol

In order to monitor the elastic performance of the structure, the SPD procedure embodies three phases, consisting of ordinary reversed cyclic displacement cycles at displacement levels smaller than FME displacement.   An initial displacement level of 25 percent of FME displacement, followed by 50 percent and 75 percent of FME for phase two and three, respectively, was used as described by Porter (1987). The displacement level of the fourth phase is increased to 100 percent of FME for the initial cycle which is followed by three degradation and three stabilization cycles. The amplitude of each consecutive decay cycle decreases by a quarter of the initial displacement. The displacement then increases to the initial displacement level and is kept constant over sufficient cycles to obtain the stabilized response of the system. Stabilized response is defined as a decrease in load between two successive cycles of not more than 5 percent.   The stabilized response is an important characteristic to assess structural performance after high wind events and during repetitive cyclic earthquake loading. Furthermore, the utilization of three cycles at the same displacement level allows the researcher to monitor the stiffness degradation of the system. For nailed wood joints and nailed shear walls, it has been determined that three stabilization cycles are sufficient to obtain a stabilized response. All following phases consist of initial, decay, and stabilization cycles.

Attributed to the high amount of cycles, which is mainly a result of the decay cycles, the energy demand of the draft ASTM standard is much higher than the true energy demand observed

in past earthquakes. It is suspected that the high number of cycles leads to failure modes such as fastener fatigue that were frequently obtained using this procedure (Heine 1997, Dolan and Johnson 1997) but have rarely been observed during earthquakes.

An additional drawback of the SPD protocol is that the displacement increments that stipulate the increase of the initial and stabilized cycles between two consecutive phases equal the yield (FME) displacement. As opposed to idealized steel material response that undergoes almost elastic plastic behavior when loaded, wood joints do not exhibit typical yield behavior. The determination of the yield point has been contentious and a wide range of definitions and methods to determine yield for wood structures has been introduced (Foliente 1996).

To address these issues, an alternative displacement function was proposed and included in the draft standard (Table 10.2). Decay cycles were omitted and the incremental displacement increase is now a function of displacement at failure derived from monotonic tests rather than yield displacement. Instead of imposing a condition of constant frequency, the alternative standard specifies a constant slip rate between 0.02 and 0.2 mm/sec.

Table 10.2: Alternate displacement protocol as proposed by the draft ASTM
standard (ASTM 1999)

Phase	Number of Cycles	Amplitude (% of $\Delta_{Failure}$)
1	1	1.25
2	1	2.50
3	1	5.00
4	1	7.50
5	1	10.00
6	3	20.00
7	3	40.00
8	3	60.00
9	3	80.00
10	3	100.00
11 – to failure	3	increase further by increments of 20% of $\Delta_{Failure}$

10.3.2 Proposed CEN Standard (prEN 12512 Draft 1996)

The draft CEN regime is displacement controlled and consists of several phases each containing up to three cycles with the same amplitude (Table 10.3). The incremental increase of the amplitudes between two consecutive phases is governed by a prior determined yield

displacement (Figure 10.4). It is suggested that the displacement at yield be determined through monotonic tests if the joint configuration is tested for the first time. Like many other standards that are being developed concurrently, the CEN provision stipulates that the rate of loading be held constant at a value between 0.02 and 0.2 mm/sec.
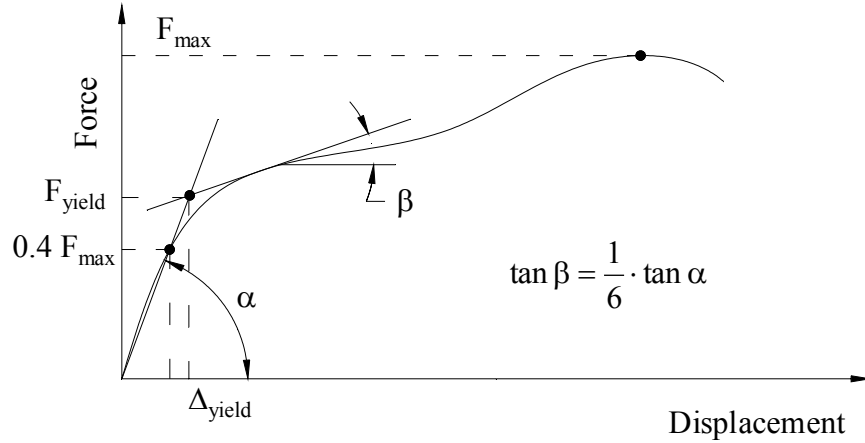

Figure 10.4: Definition of yield point for load slip curves with no well defined linear parts (prEN 1996)

Table 10.3: Proposed CEN displacement protocol

Phase	Number of Cycles	Amplitude (% of Δ_{Yield})
1	1	25
2	1	50
3	3	75
4	3	100
5	3	200
6	3	400
7	3	600
8 – to failure	3	increase further by increments of 200% of Δ_{Yield}

10.3.3 Proposed ISO Standard (Draft 1998)

As the alternate protocol proposed in the draft ASTM standard, the ISO proposal bases incremental displacement increases on fractions of the ultimate displacement rather than the displacement at yield (Foliente et al. 1998). The current ISO regime also specifies a constant rate

of slip between 0.02 and 0.2 mm/sec instead of a constant frequency. The definition of the ultimate displacement, which constitutes the mean value obtained from monotonic tests, is depicted in Figure 10.5 and the displacement protocol is revealed in Table 10.4.
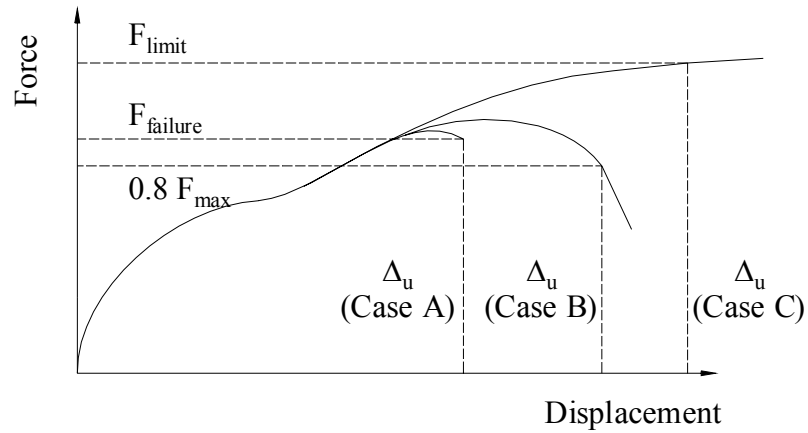
Case A: Catastrophic failure
Case B: No distinct catastrophic failure, failure load and ultimate displacement (Δ_u) are
          determined at $0.8\ F_{max}$.
Case C: No maximum load can be determined. Ultimate displacement (Δ_u) is assumed to
          be 25mm (for most joints) and maximum load equals F_{limit}.

Figure 10.5: Definition of ultimate displacement derived from monotonic loading
(after Foliente et. al 1998)

Table 10.4: Proposed ISO displacement protocol

Phase	Number of Cycles	Amplitude (% of Δ_u)
1	1	2.5
2	1	5.0
3	1	7.5
4	1	10.0
5	1	12.5
6	3	25.0
7	3	50.0
8	3	75.0
9	3	100.0
10 – to failure	3	increase further by increments of 25% of $\Delta_{Failure}$

10.3.4 ST04 - Draft New Zealand Standard

Similar to the draft standards discussed above, the proposed provision to become a testing standard assessing the performance of joints under cyclic loads in New Zealand specifies a monotonic test for new joint configurations to obtain property values that are used to adjust the cyclic displacement schedule (Shelton 1999). The test regime is equivalent to the proposed CEN protocol except the first phase is omitted (Table 10.3). The increase in amplitudes is also a function of the yield displacement, which is defined as the displacement at 0.5 F_{max}. A constant loading rate between 0.1 mm/sec and 1.5 mm/sec is specified, which is almost 8 times higher than maximum specified rates in the draft standards previously discussed.

10.3.5 CUREE-Caltech Protocol

The Consortium of Universities for Research in Earthquake Engineering (CUREE) developed a new testing protocol whose basic structure was used for all shake table and component tests of the CUREE-Caltech Woodframe Project (Krawinkler et al. 2000). Reflecting the stochastic seismic demands of earthquakes, the CUREE protocol for "deformation controlled quasi-static cyclic testing" (Krawinkler et al. 2000) contains three categories of cycles including initiation cycles, primary cycles and trailing cycles. The displacing function follows the prescribed displacement pattern listed in Table 10.5. As most of the other protocols introduced above, the CUREE protocol recommends calibration by unidirectional tests. Derived from the deformation at failure (80% F_{max}) obtained from unidirectional tests, the reference displacement, Δ, measures the deformation capacity of the specimen and is the expected sustainable displacement given the CUREE protocol has been applied. Krawinkler et al. did not give specific recommendations as to the displacement rate that should be used but referred to guidelines made by the ISO standard.

Table 10.5: CUREE displacement protocol

Phase	Number of Cycles	Amplitude (% of Δ)
1	6	5.0
2	1	7.5
3	6	5.625
4	1	10.0
5	6	7.5
6	1	20.0
7	3	15.0
8	1	30.0
9	3	22.5
10	1	40.0
11	2	30.0
12	1	70.0
13	2	52.5
14	1	100.0
15	2	75.0
10 – to failure	?	increase further by increments of 50.0% of Δ. Use two trailing cycles at 75% of initial cycle amplitude.

10.3.6 Comparison of Test Regimes

It should be recognized that, with the exception of the SPD protocol and the proposed New Zealand standard, it would take well over 50 minutes to complete a single connection test that does not fail at a slip smaller than 25 mm if the slow rates were to be used as proposed by most draft standards.

Despite the use of different input parameters obtained from monotonic test data, the draft CEN protocol, the alternative draft ASTM regime and the proposed ISO displacement function are quite similar. It stands to question whether the differences prove significant. Yasumura (1998) applied both the CEN draft standard and the draft ISO protocol to bolted joints with steel side plates. He observed little variation of results of the two regimes in terms of displacement at capacity and peak load. Numerical analysis suggests that joints in timber structures oscillate at

frequencies of 0.25 – 0.5Hz when subjected to earthquake type excitation (Chui and Ni 1995), which justifies the use of a frequency of 0.5Hz used by the SPD protocol.

Based on its scientific derivation from actual earthquake demands, the CUREE protocol was employed in this work. Another advantage of the CUREE protocol is the dependency of the displacing function on ultimate displacement rather than yield displacement making it less ambiguous and prone to variations than other standards. The SPD protocol includes decay cycles that increase the energy demand of a tested joint to unrealistic levels. Initially, the decay cycles were introduced to determine a lower bound on displacement for energy dissipation. However, with modern data acquisition available today this requirement is not deemed necessary. In view of the higher energy demand and unrealistic failure modes attributed to the high number of cycles, the use of decay cycles is controversial. A constant frequency is not desired since the rate of loading is not constant. Hence, for this study, displacing rate was fixed at 2mm/sec. The reference displacement , Δ, was estimated from monotonic tests.

10.4 Specimen Fabrication

All wood materials were gathered from locally available southern pine (graded Number 2 and better). Southern pine is a principal structural species group for the United States. Wood members were equilibrated to 12 percent moisture content prior to testing. Moisture content and specific gravity was measured for each specimen using gravimetric methods. All joint members belonging to a certain joint configuration were planed and cut to equal thickness, width and length, respectively. Bolt holes were precision-drilled using a milling machine, which resulted in minimum spacing tolerances. Lumber was bought in 12-ft lengths (3.7m) and specimens were allocated such that the minimum number of defects was located within the joint region. Because of defects, lumber utilization rate was less than 50 percent.

10.5 Discussion of Test Results

Numerical results are revealed in the next chapter in which MULTBOLT is validated. The discussion below focuses on general observations made during testing. For more detailed information, please refer to Anderson (2001).

10.5.1 Test Fixture and Displacement Protocol

The test fixture performed well. Small lag bolts or self drilling Simpson Strong-Drive ® (applied on thicker members) were sufficient to grip the wood members for all tensile loads exerted on the specimens.

Difficulties were experienced calibrating the cyclic protocol based on monotonic tests. Frequently, failure displacements observed during the limited number of monotonic tests differed greatly from those observed during cyclic experiments, which made the selection of the correct protocol difficult. Time requirements and financial resources did not permit the extension of the monotonic test program.

10.5.2 Observed Yield Modes

Lumber for the smaller members (38 x 140 mm^2) designed to yield in Mode II, was of relatively good quality and specimens could be manufactured such that no defects (knots, cracks, splits) fell within the region were the bolts were located and the minimum end distance away from the bolts. Average specific gravity of the smaller members tested was 0.57 (COV = 12.7%) which is very close to 0.55, the value reported in the literature for southern pine (AF&PA 1997). Unfortunately, most of the lumber commercially obtained for the larger members (140 x 89 mm^2) was boxed-heart lumber containing substantial portions of juvenile wood (Figure 10.6). This was also reflected in a much lower average specific gravity of 0.47 (COV = 14.3 %). In addition, probably attributed to the larger size, the material was full of drying checks often penetrating the member up to half of its thickness. While juvenile wood could not be excluded, it was attempted to keep defects such as knots, and drying cracks in particular, out of the joint region. However, owing to poor quality of the larger members and financial constraints, this could not always be accomplished and efforts were focused on keeping defects away from bolt locations.
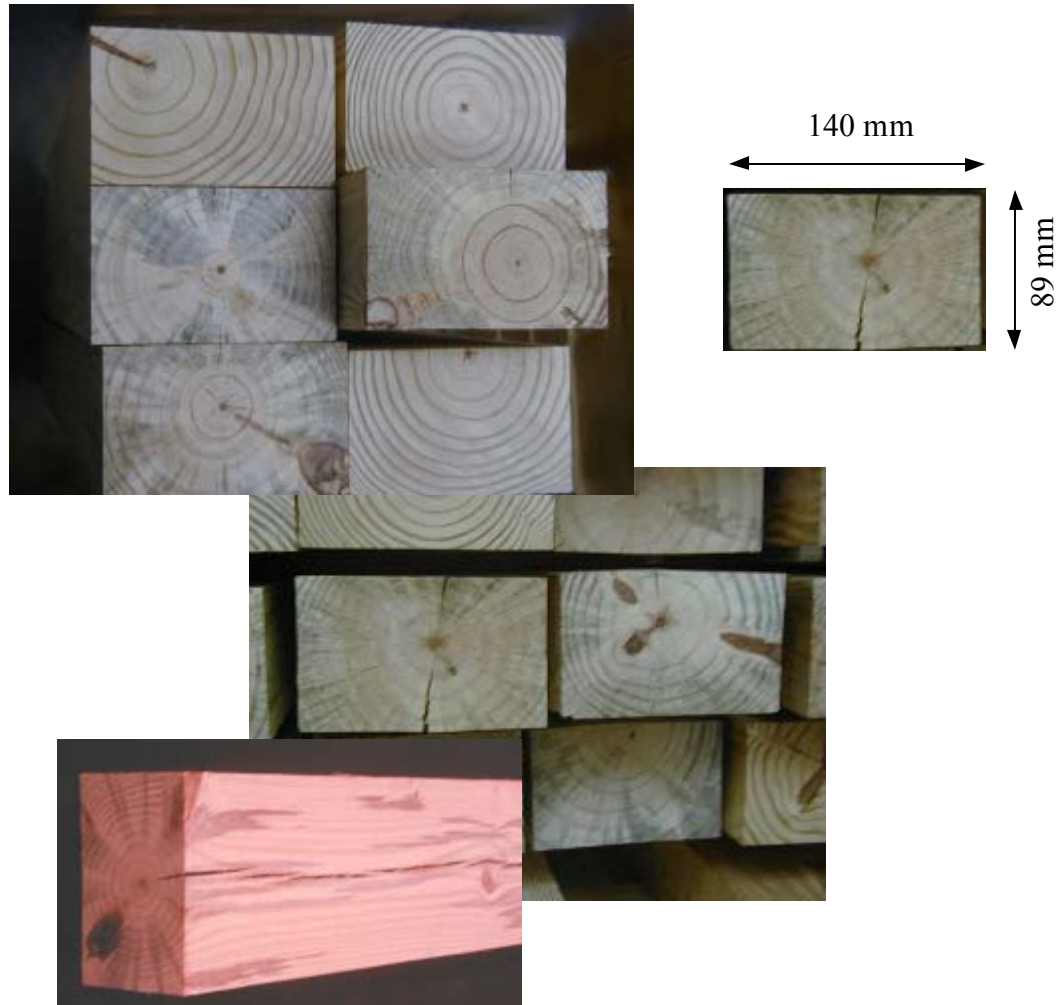
Figure 10.6: Wood used for Mode IV-type joints was boxed-heart lumber containing large proportions of juvenile wood as can be seen by the wide growth rings emanating from the pith. Despite all attempts to exclude them, micro and macro drying checks may have added to the material's variable performance.

Yield modes of single-bolt joints conformed with predicted modes. But in case of joints with thicker members, it must be emphasized that observed yield modes varied within the multiple-bolt joints tested. For example, a multiple-bolt joint predicted to yield in Mode IV by the European Yield Theory equations rarely developed Mode IV yield (Mode IV yield was only observed during monotonic tests and did not form in all fasteners). While some bolts were observed to develop a single plastic hinge and yield in Mode III, others did not develop any plastic hinge before catastrophic failure occurred (Figure 10.7). This behavior may have several causes. It is hypothesized here that in the multiple-bolt joints with larger members, the higher yield modes "evolved" from lower modes at increasing displacement amplitude. That is, the joint starts to deform like a Mode II yield, then various bolts change to Mode III and then possibly to

Mode IV. One important fact to remember is that bolt holes were drilled oversize causing all bolts initially to rotate similar to a Mode II-type deformation.

Figure 10.7: Yielded bolts and their corresponding location within the joint after cyclic tests (from Anderson (2001)). The top row shows two 5-bolt joints predicted to yield in Mode IV, but only Mode III and some Mode II yield can be observed. Middle row depicts two 3-Bolt joints predicted to yield in Mode IV. Again only Mode III and Mode II can be observed. The bottom row shows two single-bolt joints exhibiting the predicted Mode IV yield.

Figure 10.8 depicts two cases: one single-bolt joint where the bolt hole is drilled with oversize and one joint where the bolt fits tight in the hole. As soon as the joint members are displaced, the tightly fit bolt experiences pressure along the entire shaft, whereas the bolt in the oversized hole experiences no pressure until the slack introduced by hole oversize is overcome. Even after the slack is overcome, the bolt rotates and depresses a smaller area of the surrounding wood than the bolt in a tight-fit hole. If there is no oversize, the bolt starts to bend elastically about discrete points (A and B in Figure 10.8) at relatively small displacements. By contrast, holes drilled at oversize imply that the contact area of bolt and wood is much smaller and the bolt initially keeps rotating along the lines of Mode II yield until the contact area is large enough and the reaction force of the wood foundation sufficient to bend the bolt. Since the bolt spans unsupported distances brought about by hole oversize, bending does not occur at discrete points. Thus, it may be induced that, because of oversize, plastic hinges are likely to develop at larger displacements when compared to tight-fit joints. This leads to the conclusion that fasteners tend to deform in Mode II initially if bolt holes are oversized. And because the members' specific gravity and thus embedment strength values are rarely identical, plastic hinges do not form concurrently in both members. Consequently, upon rotation in Mode II, a plastic hinge may develop in one member first leading to a deformation in Mode III, at which time failure may initiate as was most often reported during tests. If premature splitting does not occur, then the bolt deforms further until finally a second plastic hinge develops. This was the case for the single-bolt joints. The reason why those joints did not fail prematurely was most likely the minimum end distance which was more than 70 percent larger than the required minimum spacing between bolts.

If we accept the above reasoning and assume a low specific gravity, low-density juvenile wood, and an allowable bolt spacing of more than 40 percent less than minimum end distance, then it becomes clear why yield modes did not follow predictions and actually varied per fastener within members. Because bolts have the initial tendency to deform according to Mode II, stresses may already reach material strength, especially in juvenile wood, and the material may fail before higher yield modes are achieved. Moreover, since the contact area is smaller due to hole oversize, Mode IV yield is less likely to develop. Add to it a lower embedment strength because of less dense material and juvenile wood, and the probability of a Mode IV yield is reduced even further. In addition, as a result of manufacturing tolerances and material deformation, not all fasteners displace an equal amount within a multiple-bolt joint. This may cause some fasteners to develop higher yields such as Mode III but others may still rotate in Mode II. The relatively

small allowable spacing increases the probability of premature splitting, which further reduces chances to observe higher yield modes.

It should be noted that the yield mode development as hypothesized above is most likely a peculiarity of single shear joints and probably does not occur in the same fashion in three-member, double shear joints, because, owing to their geometry, these joints do not yield in Mode II. Double shear joints yield in either Mode I, III, or IV. Yielding should start in Mode I, evolve to Mode III and finally arrive at Mode IV. But if yielding in Mode I, the fastener experiences foundation forces along its entire shaft and deformation is similar to a simple beam under distributed load. The contrast to two-member joints is that the bolt is in full contact with the bolt hole surface of the middle member and spans a small free distance in the side member. Thus, Mode IV yield is more likely to develop in double shear joints than in single shear joints if holes are drilled oversize.
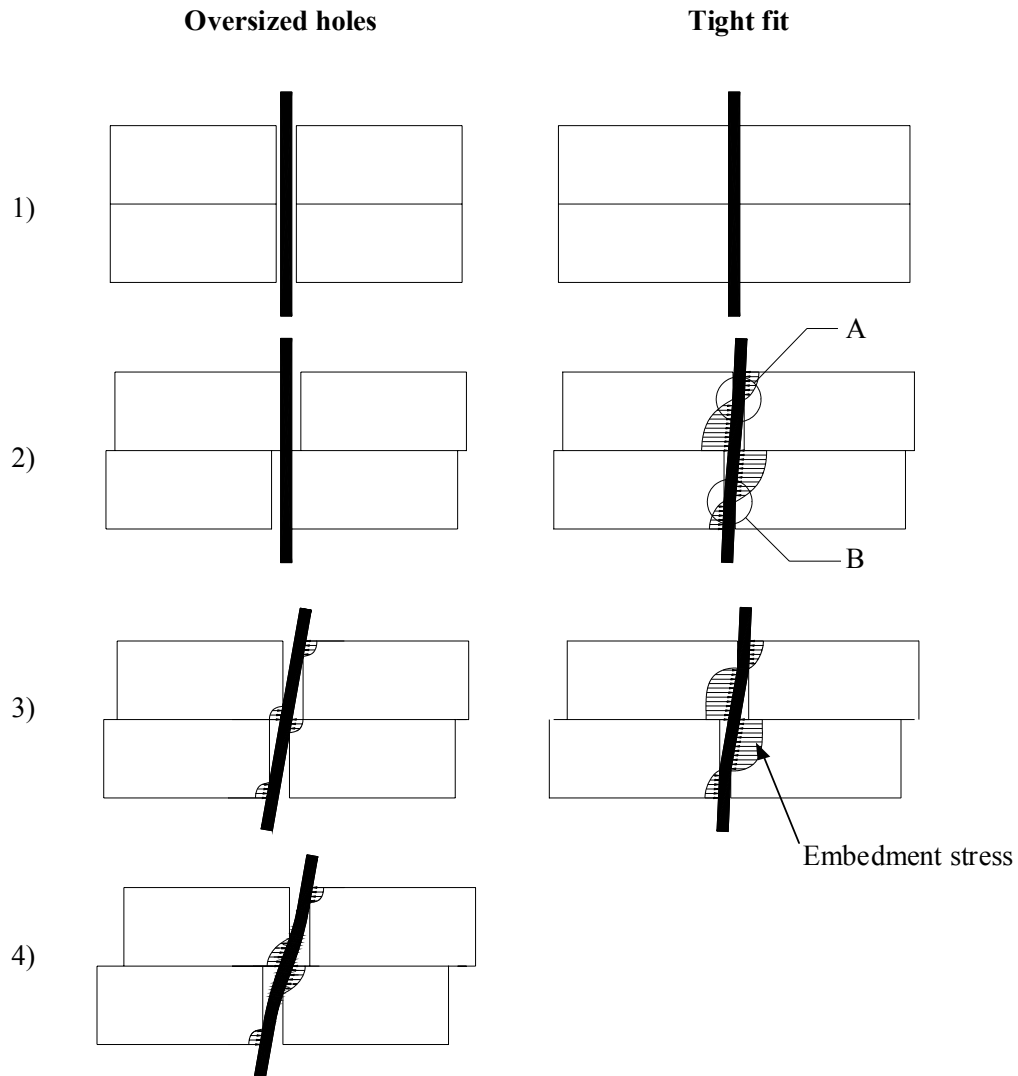
Oversized holes   **Tight fit**

Figure 10.8: Comparison of displaced joint with oversized hole to a joint where the bolt sits tight in the hole.

10.5.3 Observed Failure Modes

10.5.3.1 Mode II Yield

Joints yielding in Mode II exhibited brittle failure. A single crack emanating from the bolt hole initiated failure of single-bolt joints in almost all specimens. Because only one crack formed, failure was most likely caused by perpendicular-to-grain tensile stresses. On two single-

bolt specimens, failure triggered by shear stresses was detected. Shear failure is portrayed as two cracks running a distance apart parallel to the grain.

Tension perpendicular-to-grain stresses triggered failure in most multiple-bolt joints. Once a crack formed, it rapidly propagated along the specimen. It should be noted, however, that although a single crack most often split the entire joint region, it almost never ran along the centerline of the joint (Figure 10.9). This supports the hypothesis that interface friction between bolt and wood produces essentially two crack planes left and right of the joint centerline perpendicular to the shear plane (see Section 2.1.3.1.1). Further substantiating the crack plane hypothesis was the observation of shear failure on a few specimens. In particular, failure was initiated by two cracks forming between fasteners (left and right from the centerline of the joint) (Figure 10.10).

No difference in failure modes was detected between unidirectionally and cyclically stressed specimens.

Figure 10.9: Failure initiated by a single crack due to tension perpendicular-to-grain stresses. Note that the crack does not run through the centerline of the joint (from Anderson (2001)).
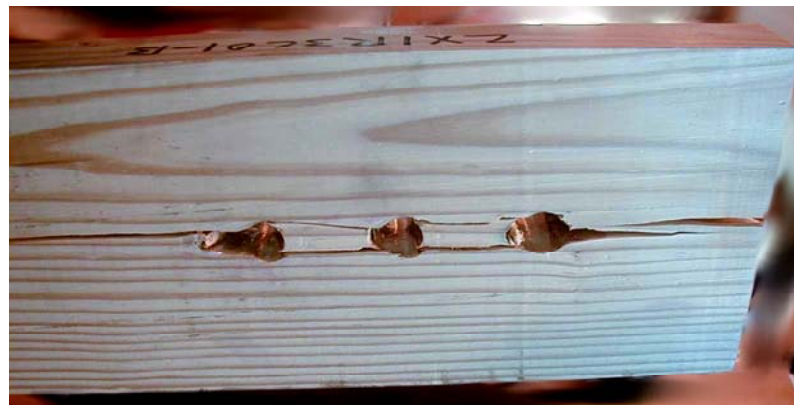

Figure 10.10: Shear failure as is evident by two cracks between fasteners (from Anderson (2001)).

10.5.3.2 Specimens Predicted to Yield in Mode IV

Some single-bolt joints yielding in Mode IV did not fail catastrophically but failure occurred on account of wood crushing underneath the bolt and fastener bending. In addition, because of large deformations, washers and bolt heads were pressed considerably into the side members indicating that substantial tensile forces developed in the fastener. Despite the joint yielding in a more ductile manner, brittle failure was detected on a few specimens, where a crack formed in at least one side member. Since almost all single-bolt joints exhibited Mode IV yield, however, cracks developed at relatively large deformation (Figure 10.11).

Figure 10.11: Failure mode in single-bolt Mode IV specimens was primarily wood crushing. Still, at larger displacement brittle failure was frequently detected (from Anderson (2001)).

Similar to Mode II-type specimens, multiple-bolt joints designed to yield in Mode IV exhibited brittle failure due to tension perpendicular-to-grain stresses and shear stresses. However, shear failure was much more frequent compared to Mode II-type joints, which may be attributed to the lower-density lumber and the lower-strength juvenile wood.
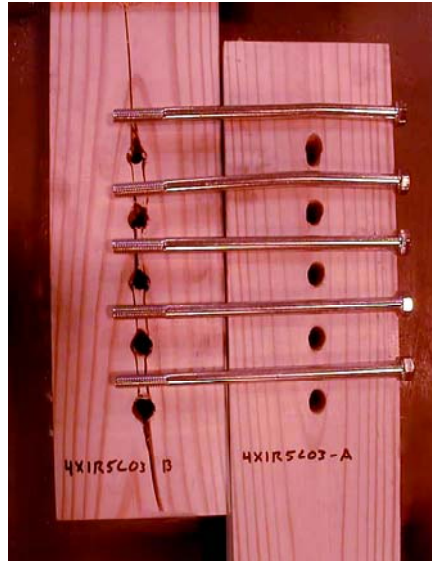
Figure 10.12: Failure initiated by shear stress on joint designed to yield in Mode IV, but Mode II and III yield was observed.